URSI GASS 2021, Rome, Italy, 28 August - 4 September 2021

Beamforming Approach for Steerable Null Synthesis in a Four-Element Conformal Array fed with a Radio-Frequency Reconfigurable Network

Valentina Palazzi(1), Federico Alimenti(1), Luca Roselli(1), and Paolo Mezzanotte(1)
(1) University of Perugia, Perugia, Italy, 06125, https://www.unipg.it/

Abstract

This paper presents a beamforming network used to synthesize steerable nulls. The antenna topology consists of four patch antennas placed on the lateral sides of a cube. From the analysis of the array factor and the radiation pattern of the single radiating elements, the theory to realize fully steerable nulls on the azimuth plane is presented. The array, targeted for an operating frequency of 3.6 GHz, is fed by a reconfigurable radio-frequency network. The network, which bases its reconfigurability on eight phase shifters, makes it possible to excite couples of adjacent output ports with arbitrary amplitudes and phases. The radiation pattern of the topology is measured for different excitations, confirming the theory. This approach opens the way to a new beamforming approach, that can be applied to interference removal and radio localization applications.

1 Introduction

With the advent of 5G, and the migration toward higher operating frequencies, an interest for low-cost compact reconfigurable antenna systems has emerged. Antennas able to reconfigure their radiation pattern on-demand can be profitably used both in telecommunications and in sensing applications [1].

In beamforming studies, antenna systems with null steering capabilities have played a crucial role. Nulls can be used to shape the beam, so that the information is transmitted only towards the intended recipients, and can be used to avoid interference problems. Indeed, as the number of users is rapidly growing, there is a risk of receiver jamming caused by strong signals coming from different directions. This risk can be mitigated generating a null in the radiation pattern of the antenna at the direction of the interference. Null synthesis is also at the base of radar systems used for tracking, and for radio localization.

Approaches for null synthesis have been investigated for different array configurations, with the aim to reduce the feed network complexity and improve flexibility. For instance, in [4] null steering was performed in a linear array controlling the complex weights of the two side elements of the array. [2] proposed a null-steering approach for planar arrays based on the control of the excitations of edge elements placed along the symmetrical axes of the array. In [3] a technique is proposed based on genetic algorithm and Schelkunoff nulling theory to achieve fast steering of the main beam and nulls in a circular array.

To perform null synthesis a feed network able to modify amplitude and phase relations among its output ports is usually needed. The most traditional approach consists of using phase shifters and attenuators/amplifiers at the output ports (at least in a subset of them). The latter ones can cause consistent power loss and matching issues in case high dynamic ranges are required.

In this paper a beamforming approach for a conformal four-element array is presented. The array is fed with a reconfigurable 1×4 power distribution network, able to excite each couple of adjacent radiating elements with arbitrary amplitude and phase relations. A simplified version of the matrix was already used in [5], where, however, the activated output signals were equal-magnitude, and signals could be either in phase or 180° out of phase. The developed theory is finally validated by an experimental campaign, and conclusions are drawn.

2 Theoretical Analysis

2.1 Antenna Topology

This section describes an approach to synthesize nulls at arbitrary directions on a plane, based the analysis of the array factor of the proposed topology and on the radiation pattern of each radiating element.

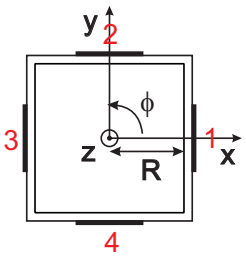

Figure 1. Top view of the proposed antenna topology.

The considered antenna topology consists of four rectangular patch antennas, placed on the lateral sides of a cube. The radiating elements are aligned with the x and y axis, as

shown in Fig. 1. The side of the cube is $\lambda_0/2$ at the operating frequency, where λ_0 is the free-space wavelength.

The field generated by a generic array in the far zone, $\mathbf{E}(\mathbf{r})$, is given by

$$\mathbf{E}(\mathbf{r}) = \mathbf{f}(\theta,\phi)\frac{e^{-jk_0 r}}{4\pi r}\sum_{i=1}^{n} C_i e^{j\alpha_i + jk_0 \mathbf{a_r}\cdot\mathbf{r_i}}, \qquad (1)$$

where $\mathbf{f}(\theta,\phi)$ is the electric-field radiation pattern of the single radiating element, $k_0 = 2\pi/\lambda_0$ is the propagation constant, C_i and α_i are the amplitude and phase of excitation of the i-th radiating element, and $\mathbf{r_i}$ is the position vector of the i-th element. The sum term in (1) is the array factor, $\mathbf{F}(\theta,\phi)$, which depends on the relative position of the radiating elements and their excitations. The proposed topology can be used to perform beamforming on the azimuthal plane of the array (i.e., the xy plane), where $\theta = \pi/2$. Therefore, the study of the radiation pattern of the array is limited to the xy plane. On this plane, the unit vector of the radial distance $\mathbf{a_r}$ simplifies as follows:

$$\mathbf{a_r} = \mathbf{a_x}\cos\phi + \mathbf{a_y}\sin\phi. \qquad (2)$$

The position vectors for the four elements are $\mathbf{r_1} = \mathbf{a_x}R$, $\mathbf{r_2} = \mathbf{a_y}R$, $\mathbf{r_3} = -\mathbf{a_x}R$, $\mathbf{r_4} = -\mathbf{a_y}R$, respectively, where R is the antenna distance from the origin, equal to $\lambda_0/4$.

The array factor for the specific antenna geometry becomes

$$\begin{aligned}\mathbf{F}(\theta=\pi/2,\phi) = {} & C_1 e^{j\alpha_1 + j\frac{\pi}{2}\cos\phi} + C_2 e^{j\alpha_2 + j\frac{\pi}{2}\sin\phi} \\ & + C_3 e^{j\alpha_3 - j\frac{\pi}{2}\cos\phi} + C_4 e^{j\alpha_4 - j\frac{\pi}{2}\sin\phi}. \qquad (3)\end{aligned}$$

The co-polar radiation pattern of a single rectangular patch has a maximum in the broadside direction, a half power beam-width of about 90°, and it has negligible values in the half plane below its ground plane. Therefore, we can assume that the radiation pattern in each of the four quadrants of the plane depends only on the two adjacent patch antennas.

Without loss of generality, the first quadrant, corresponding to $0° < \phi < 90°$, is analyzed. For simplicity we firstly assume that the radiation pattern of the single radiating element is constant in the quadrant (this assumption will be removed later on). To obtain a null in the radiation pattern, the following condition must be verified:

$$C_1 e^{j\alpha_1 + j\frac{\pi}{2}\cos\phi} + C_2 e^{j\alpha_2 + j\frac{\pi}{2}\sin\phi} = 0. \qquad (4)$$

If $C_1 = C_2$, (4) is verified when the phases of the two complex exponentials differ by odd multiples of π, as follows:

$$\alpha_1 + \frac{\pi}{2}\cos\phi + (n+1)\pi = \alpha_2 + \frac{\pi}{2}\sin\phi, \qquad (5)$$

where $n = 0, 1, \ldots$. For simplicity, $n = 0$ is chosen. From (5), the phase difference between the antenna excitations can be derived:

$$\Delta\alpha = \alpha_2 - \alpha_1 = \frac{\pi}{2}(\cos\phi - \sin\phi) + \pi. \qquad (6)$$

Therefore, for each angle ϕ in the interval of interest, we can obtain the phase difference $\Delta\alpha$ between the excitations of the two adjacent radiating elements corresponding to a null in that particular direction, as shown in Fig. 2. As expected, the two radiating elements must be fed with

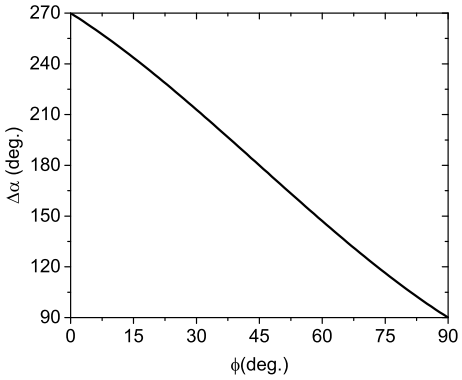

Figure 2. Phase difference between the excitations of the two adjacent radiating elements of the first quadrant corresponding to a null in a direction ϕ.

equal-magnitude 180°-out-of-phase signals to obtain a null at $\phi = 45°$, as already demonstrated in [5].

In practice, the field radiated by the single patch is not constant with ϕ: for a given ϕ different from 45°, the magnitude of the radiation pattern associated with the two adjacent radiating elements is different. In Fig. 3 the simulated radiation patterns of the two patch antennas are shown. For $\phi = 60°$ (highlighted in black) the radiation pattern of antenna 1 is almost 4 dB below the radiation pattern of antenna 2. Therefore, C_1 and C_2 must be varied to compensate for this difference.

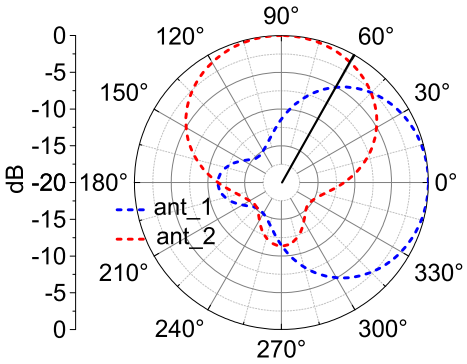

Figure 3. Simulated radiation patterns of two adjacent patches fed individually.

2.2 Feed network

To realize a steerable null with the proposed antenna topology, a reconfigurable feed network must be used, able to feed each couple of adjacent radiating elements with different relative amplitudes and phases, while preserving matching at all ports.

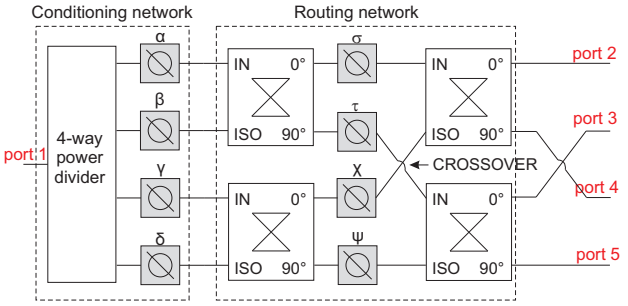

Figure 4. Schematic of the adopted 1×4 reconfigurable feed network.

To this purpose, the feed network shown in Fig. 4 is used. The circuit, which includes a conditioning network, based on one 4-way power divider and four variable phase shifters α, β, γ, and δ, and a routing network, based on four branch-line couplers and other four variable phase shifters σ, τ, χ and ψ, was firstly presented in [6]. The input signal at port 1 is distributed to the whole circuit, and the variable phase shifters are used to modify the phase relation among the different paths. This is shown by the transmission coefficients of the network, each of which is the sum of four complex terms, as follows:

$$S_{21} = \frac{1}{4}\left[e^{-j(\alpha+\sigma)} - je^{-j(\beta+\sigma)} - je^{-j(\gamma+\chi)} - e^{-j(\delta+\chi)}\right], \tag{7}$$

$$S_{31} = \frac{1}{4}\left[-je^{-j(\alpha+\tau)} + e^{-j(\beta+\tau)} - e^{-j(\gamma+\psi)} - je^{-j(\delta+\psi)}\right], \tag{8}$$

$$S_{41} = \frac{1}{4}\left[-je^{-j(\alpha+\sigma)} - e^{-j(\beta+\sigma)} + e^{-j(\gamma+\chi)} - je^{-j(\delta+\chi)}\right], \tag{9}$$

$$S_{51} = \frac{1}{4}\left[-e^{-j(\alpha+\tau)} - je^{-j(\beta+\tau)} - je^{-j(\gamma+\psi)} + e^{-j(\delta+\psi)}\right]. \tag{10}$$

This way, changing the values of the eight phase variables, α, β, γ, δ, σ, τ, χ and ψ, the magnitude and phase relations among the signals at ports 2-5 can be varied dynamically. It can be demonstrated that

$$|S_{21}|^2 + |S_{31}|^2 + |S_{41}|^2 + |S_{51}|^2 = 1. \tag{11}$$

regardless of the values assumed by the phase variables. This means the overall power transmitted from the input to the output ports is the same for each output signal configuration, which is a significant advantage to the more traditional beamforming networks, based on attenuators/amplifiers and phase shifters.

With respect to the circuit in [6], an additional crossover is used to invert ports 3 and 4. This is done to avoid the phase limitations experienced when the two activated output ports are connected to the same output branch-line coupler (in this case ports 2-4 and ports 3-5). In [6] it is observed that they can be only in phase or 180° out of phase. Thanks to the crossover, these ports are not adjacent. Therefore, we can use the network to change amplitude and phase relations between each couple of adjacent output ports arbitrarily. Note that, since the array is circular, port 2 is adjacent to port 5.

3 Experimental Results

The feed network described in Sec. 2.2 is realized in microstrip technology, and the prototype used for the measurement is shown in Fig. 5 [6]. Two-section switched-line phase shifters cascaded in linear sequence are used to implement the phase variables. The electrical length of each line section is described in [6]. The circuit, targeted for 3.6 GHz, is realized with a multi-layer PCB based on two 500μm thick Rogers 4350B laminates stacked on each side of a prepreg layer. The top layer is dedicated to the radio-frequency components, while the bottom layer is dedicated to the dc connections between the single-pole double-through switches of the phase shifters and the DIP switches used to control their connection to the supply voltage (2.2 V). The output crossover is simply implemented

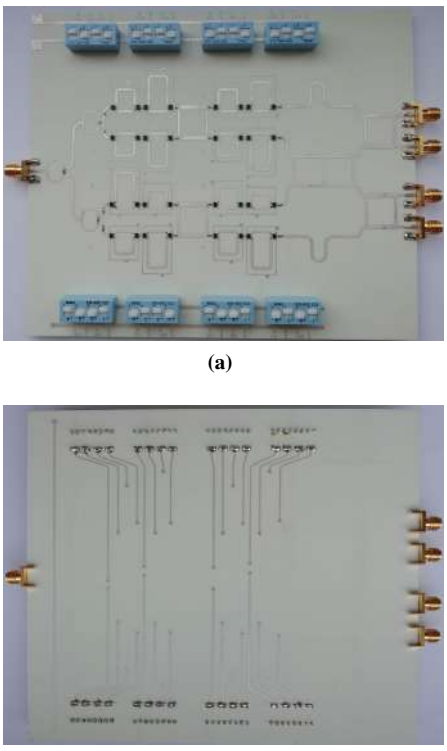

(a)

(b)

Figure 5. Photo of the matrix prototype: (a) top view and (b) bottom view [6].

crossing the cables that connect the feed network to the antenna topology.

The adopted experimental setup is illustrated in Fig. 6. The radiating elements of the array are resonant rectangular patch antennas, which are linearly polarized and matched to 50 Ω. The radiation pattern of the antenna topology is measured in the far-field region in a laboratory environment.

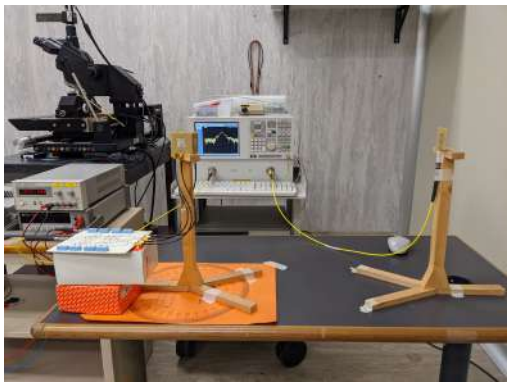

Figure 6. Experimental setup.

The network is used to excite antennas 1 and 2 with different amplitudes and phases in order to steer the null in the first quadrant. The following cases are tested:

- $C_1 = 0.707$, $C_2 = 0.707$, $\Delta\alpha = 180°$, corresponding to a null at $\phi = 45°$. This is realized setting the following phase variables: $\alpha = 180°$, $\beta = 0°$, $\gamma = 0°$, $\delta = 180°$, $\sigma = 0°$, $\tau = 0°$, $\chi = 90°$, $\psi = 90°$.
- $C_1 = 0.577$, $C_2 = 0.816$, $\Delta\alpha = 225°$, corresponding to a null at $\phi = 30°$. This is realized setting the following phase variables: $\alpha = 0°$, $\beta = 160°$, $\gamma = 250°$, $\delta = 270°$, $\sigma = 135°$, $\tau = 90°$, $\chi = 45°$, $\psi = 180°$.
- $C_1 = 0.316$, $C_2 = 0.949$, $\Delta\alpha = 270°$, corresponding to a null at $\phi = 0°$. This is realized setting the following phase variables: $\alpha = 90°$, $\beta = 160°$, $\gamma = 250°$, $\delta = 0°$, $\sigma = 90°$, $\tau = 180°$, $\chi = 0°$, $\psi = 270°$.

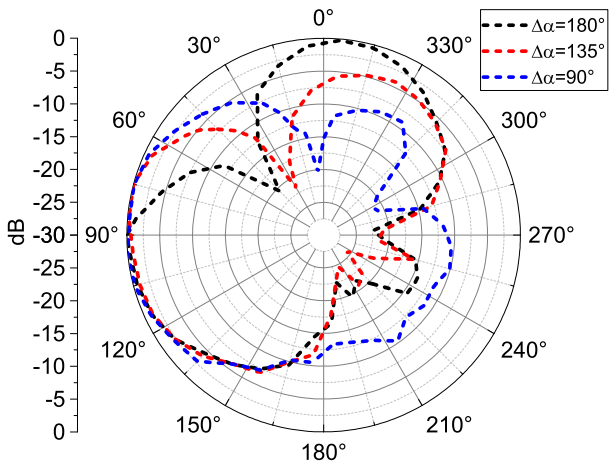

Figure 7. Measured notmalized radiation patterns on the *xy* plane for different excitations.

The normalized measured copolar radiation patterns on the azimuthal plane (*xy* plane) are shown in Fig. 7. The nulls are observed at the expected ϕ angles. As expected, the lobe associated with the antennas closer to the null is smaller than the other: this is due to the fact that this antennas is fed with less power. If more balanced lobes are needed, a beamforming strategy involving also a third radiating element (in this case antenna 4) must be implemented.

4 Conclusions

An antenna topology, based on four patch antennas placed on the lateral sides of a cube, has been presented. Firstly, the array factor for the topology is derived, together with the approach to synthesize steerable nulls on its azimuthal plane. The main features of the reconfigurable network used to feed the antenna have been presented. The network, based on a 4-way power divider, four branch-line couplers and eight phase shifters, proved to be able to excite couples of adjacent radiating elements with arbitrary amplitude and phases. A proof-of-concept prototype has been manufactured and tested, able to steer a null on the azimuthal plane, thereby proving the capability of the system to be applied for interference removal and radio localization.

5 Acknowledgements

This paper is part of the ADACORSA project that has received funding within the Electronic Components and Systems for European Leadership Joint Undertaking (ECSEL JU) in collaboration with the European Union's H2020 Framework Programme (H2020/2014-2020) and National Authorities, under grant agreement 876019.

References

[1] Godfrey Anuga Akpakwu, Bruno J. Silva, Gerhard P. Hancke, and Adnan M. Abu-Mahfouz. A Survey on 5G Networks for the Internet of Things: Communication Technologies and Challenges. *IEEE Access*, 6:3619–3647, 2018.

[2] Soumyo Chatterjee, Sayan Chatterjee, and Arijit Majumdar. Edge element controlled null steering in beam-steered planar array. *IEEE Antennas Wireless Propag. Lett.*, 16:2521–2524, 2017.

[3] Abubakar Hamza and Hussein Attia. Fast Beam Steering and Null Placement in an Adaptive Circular Antenna Array. *IEEE Antennas Wireless Propag. Lett.*, 19(9):1561–1565, sep 2020.

[4] Jafar Ramadhan Mohammed and Khalil Hassan Sayidmarie. Null steering method by controlling two elements. *IET Microwaves, Antennas & Propagation*, 8(15):1348–1355, dec 2014.

[5] Valentina Palazzi. Phase-controlled beamforming network intended for conformal arrays. *URSI Radio Science Bulletin*, 2020(373):12–21, jun 2020.

[6] Valentina Palazzi, Federico Alimenti, Paolo Mezzanotte, and Luca Roselli. Novel Magnitude and Phase Reconfigurable 1 × 4 RF Power Distribution Network. *IEEE Trans. Microw. Theory Techn.*, 69(1):29–42, January 2021.